

Quenching of the quantum Hall effect in a uniform ballistic quantum wire

This article has been downloaded from IOPscience. Please scroll down to see the full text article.

1993 J. Phys.: Condens. Matter 5 L397

(<http://iopscience.iop.org/0953-8984/5/33/004>)

View [the table of contents for this issue](#), or go to the [journal homepage](#) for more

Download details:

IP Address: 171.66.16.96

The article was downloaded on 11/05/2010 at 01:37

Please note that [terms and conditions apply](#).

LETTER TO THE EDITOR

Quenching of the quantum Hall effect in a uniform ballistic quantum wire

D P Chu† and P N Butcher

Department of Physics, University of Warwick, Coventry CV4 7AL, UK

Received 28 May 1993

Abstract. Self-consistent calculations are made of wave functions and two kinds of Hall resistance for a 2DEG confined in a uniform ballistic quantum wire in a weak perpendicular magnetic field when several subbands are occupied. We find intermittent quenching of the Hall resistance associated with the local chemical potential as the electron density varies. The quenching is due to the overlap of opposite-going wave functions in the same subband, which is enhanced significantly by the singularity of the density of states at the subband minimum as well as by Coulomb interactions between electrons.

In the last decade, magnetotransport in semiconductor microstructures has been intensively investigated and many interesting phenomena have been observed [1]. Recently, particular attention has been given to the behaviour in weak magnetic fields, e.g. quenching of the quantum Hall resistance (QHR) [2-5], the last Hall plateau [2-5], and the bend resistance in a four-terminal case [6-8]. Much theoretical effort has been devoted to understanding these phenomena. Microscopic calculations of a quasi-one-dimensional (Q1D) electron gas model which ignored the significance of the density of states and Coulomb interaction effects in the weak-coupling limit failed to show quenching [9,10]. Self-consistent calculations of the QHR associated with the electrostatic potential gave only a linear dependence on magnetic field as in the classical case [11]. In the strong coupling regime, quenching of the QHR has been obtained theoretically when there are resonant states involved [12,13]. Other investigations suggest that quenching is due to a geometrical property of the structure and is not intrinsic to the Q1D limit even with strongly coupled probes [14]. They also demonstrate that smoothing the corners of the structure suppresses the QHR [15]. Assuming a realistic confining potential with soft boundaries provides a detailed explanation of many experimental results via classical trajectories [16]. However, very recent experimental results show that there *is* quenching of the QHR of a quantum wire in the weak-coupling limit [17].

In this letter we present self-consistent calculations of the QHR R_{LCP} associated with the local chemical potential (LCP) in a uniform ballistic wire. The following specific results are obtained: (1) quenching of R_{LCP} is intrinsic in the weak coupling limit, (2) it is due to the overlap of opposite-going wave functions, (3) quenching happens intermittently as the electron density increases, and (4) the QHR associated with the electrostatic Hall potential (EHP) is closely linear in the magnetic field B in spite of subband depopulation effects.

† On leave from the Institute of Physics, Chinese Academy of Sciences, Beijing 100080, People's Republic of China.

Before we go into detail, let us first distinguish two kinds of intrinsic Hall resistance in a quantum wire. One is R_{EHP} , defined as the EHP difference between the two edges of a wire divided by the total current passing through the two terminals. The other, R_{LCP} , is obtained by using the LCP difference across the wire instead of the EHP. The EHP is the potential induced by the electrons in the wire to balance the Lorentz force, while the LCP is defined as the chemical potential of a reservoir which is connected non-invasively at a particular point in the wire when no net current flows through the contact. We believe that the potential difference measured by conventional weak-coupling current-stopping procedures (as discussed by Engquist and Anderson [18] and Landauer [19]) is the LCP difference. We show in the following that it is R_{LCP} which is quenched in a weak magnetic field. R_{EHP} retains the linear dependence on magnetic field which occurs in classical theory.

The system to be considered is a 2DEG with electron density n_s confined in a space of width W in the x - y plane by infinite potential barriers at $y = \pm W/2$. A uniform magnetic field B is applied in the z direction and described in the Landau gauge by writing the vector potential as $A = (-By, 0, 0)$. Following previous authors [20, 11] and a recent paper by the present authors [21], we introduce an EHP $V(y)$ which is induced by the external magnetic field. The electron wave function $\psi_n(x, y)$ satisfies the Schrödinger equation

$$\left[(1/2m^*) (p + eA)^2 + (-e)V(y) \right] \psi_n(x, y) = E_n \psi_n(x, y)$$

where m^* is the effective mass and n is the index of the subbands ($n = 0, 1, 2, \dots$ refers to the lowest, the second, the third, ... subbands). The normalized eigenfunctions are then of the form $\psi_n(x, y) = L_x^{-1/2} \exp(ik_x x) \chi_{n,k_x}(y)$, where L_x is the length of the wire. The EHP, which must be determined self-consistently, can be expressed as

$$V(y) = \begin{cases} \frac{1}{4\pi\epsilon_0\epsilon} \int_{-W/2}^{W/2} dy' (-2 \ln |y - y'|) \delta\sigma(y') & -W/2 \leq y \leq W/2; \\ -\infty & \text{otherwise.} \end{cases}$$

The redistribution of the electron charge density $\delta\sigma(y)$ is

$$\delta\sigma(y) = -\frac{e}{2\pi} \sum_{n,\sigma} \int_{k_{-x,E_F-\Delta/2}^{(n)}}^{k_{x,E_F+\Delta/2}^{(n)}} dk_x [|\chi_{n,k_x}(y)|^2 - |\chi_{n,k_x}^{(0)}(y)|^2]$$

where $k_{x,E_F+\Delta/2}^{(n)}$ and $k_{-x,E_F-\Delta/2}^{(n)}$ are the Fermi wave numbers of subband n for the positive and the negative x directions respectively, Δ is the chemical potential difference between the two terminals, and σ is the spin label. We make Δ small enough to ensure that we stay in the linear transport regime. The functions $\chi_{n,k_x}^{(0)}(y)$ are the eigenfunctions of the Schrödinger equation in the absence of a magnetic field [20, 11]. To complete the calculation, we need to constrain E_F in the Fermi wave numbers so as to yield the given electron density n_s for fixed Δ , i.e.

$$n_s = \frac{1}{2\pi W} \sum_{n,\sigma} [k_{x,E_F+\Delta/2}^{(n)} - k_{-x,E_F-\Delta/2}^{(n)}].$$

The current density distribution across the wire can then be calculated from

$$j_x(y) = -\frac{e\hbar}{2\pi m} \sum_{n,\sigma} \int_{k_{-x,E_F-\Delta/2}^{(n)}}^{k_{x,E_F+\Delta/2}^{(n)}} dk_x \left(k_x - \frac{1}{l_B^2} y \right) \chi_{n,k_x}^2(y)$$

where $l_B = (\hbar/eB)^{1/2}$ is the magnetic length. Since the total current is $I_x = \int dy j_x(y)$, the longitudinal resistance R_L can also be calculated straightforwardly. The LCP $U(y)$ may also be calculated from the formula [22, 23]

$$eU(y) = \frac{\sum_{n,\sigma} [\mu_1 |\chi_{n,k_x,E_F+\Delta/2}(y)|^2 + \mu_2 |\chi_{n,k_x,E_F-\Delta/2}(y)|^2] / v_n}{\sum_{n,\sigma} [|\chi_{n,k_x,E_F+\Delta/2}(y)|^2 + |\chi_{n,k_x,E_F-\Delta/2}(y)|^2] / v_n}$$

where μ_1 (μ_2) is the chemical potential of the reservoir connected at the left (right) end of the wire, $\chi_{n,k_x,E}(y)$ and $\chi_{n,k_x,E}(y)$ are the right- and left-going electron wave functions respectively, and v_n is the velocity at Fermi level. We notice that there is a difference between the formula of local chemical potential given above and the formula used in [9] and [10] where the factor v_n^{-1} for the density of states at Fermi level is not included. This difference is the primary reason why there is no quenching in their results.

When the above equations are solved we obtain self-consistent electron wave functions, the distributions of the EHP and the LCP across the wire and two kinds of intrinsic Hall resistance, R_{EHP} and R_{LCP} . To interpret the physics revealed in the results it is useful to have representations of the electron distributions in the subband wave functions. We therefore define a convenient mean position $\langle y_n \rangle$ and a half-width $\langle (\Delta y_n^2) \rangle^{1/2}$ in subband n and cross hatch the region lying between $\langle y_n \rangle - \langle (\Delta y_n^2) \rangle^{1/2}$ and $\langle y_n \rangle + \langle (\Delta y_n^2) \rangle^{1/2}$ to indicate the spread of wave functions. We take $\langle y_n \rangle = \langle n | y | n \rangle$ and $\langle (\Delta y_n^2) \rangle = \langle n | y^2 | n \rangle - \langle y_n \rangle^2$. However, when $n > 0$, in evaluating $\langle y_n \rangle$ and $\langle (\Delta y_n^2) \rangle$ we keep only the renormalized part of the wave function lying between a side wall and the node closest to it. This procedure has the merit of producing useful pictorial representations of the electron distributions in the excited subband wave functions while avoiding unhelpful complications due to the nodes, and gives a better description of the behaviour of the electron wave functions near the edges, which is what determines R_{LCP} . In our numerical calculations, we always use the parameters of a GaAs wire [11] of width $w = 100$ nm and we ignore the Zeeman splitting which is a reasonable first approximation in a model calculation for a GaAs system.

Figure 1(a) shows plots against B which indicate the degree of overlap of the oppositely propagating wave functions in the ground subband when $n_s = 2 \times 10^{14} \text{ m}^{-2}$. For this electron density only the ground subband is occupied. In this case, the formula for the LCP becomes very simple and the density-of-states factor cancels out. The departure of the QHR from its quantized value is, therefore, entirely due to the overlap of opposite-going wave functions. Data for $\langle y_0 \rangle$ and the wave function spread are given by the up (down) triangles and the cross-hatch lines sloping down to the right (left) for right (left)-going wave functions respectively. Figure 1(b) gives data for R_L (crosses), R_{EHP} (squares), and R_{LCP} (circles) for the same value of n_s . We see that R_{LCP} increases rapidly as the opposite-going wave functions begin to separate and remains at the quantized value when they are well separated at the two edges of the wire.

Figures 1(c)–(e) show corresponding plots when $n_s = 4 \times 10^{14} \text{ m}^{-2}$. For this density two subbands are occupied when $B < 0.5$ T but only the ground subband is occupied when $B > 0.5$ T. We chose this n_s to make the Fermi wave number of the uppermost occupied subband much smaller than the others when $B \rightarrow 0$ so that the Fermi level is very close to the bottom of this subband, which is flat. Consequently, the closer the Fermi level is to the bottom of a subband the larger is the density of states of that subband at the Fermi level. In this situation, the LCP difference between the two edges of the wire is greatly reduced by both the large overlap of the opposite-going wave functions at low B and the significant increase of the density of states of the uppermost occupied subband. Figures 1(c) and (d) show the degree of overlap in the $n = 0$ and $n = 1$ subbands respectively. Figure 1(e)

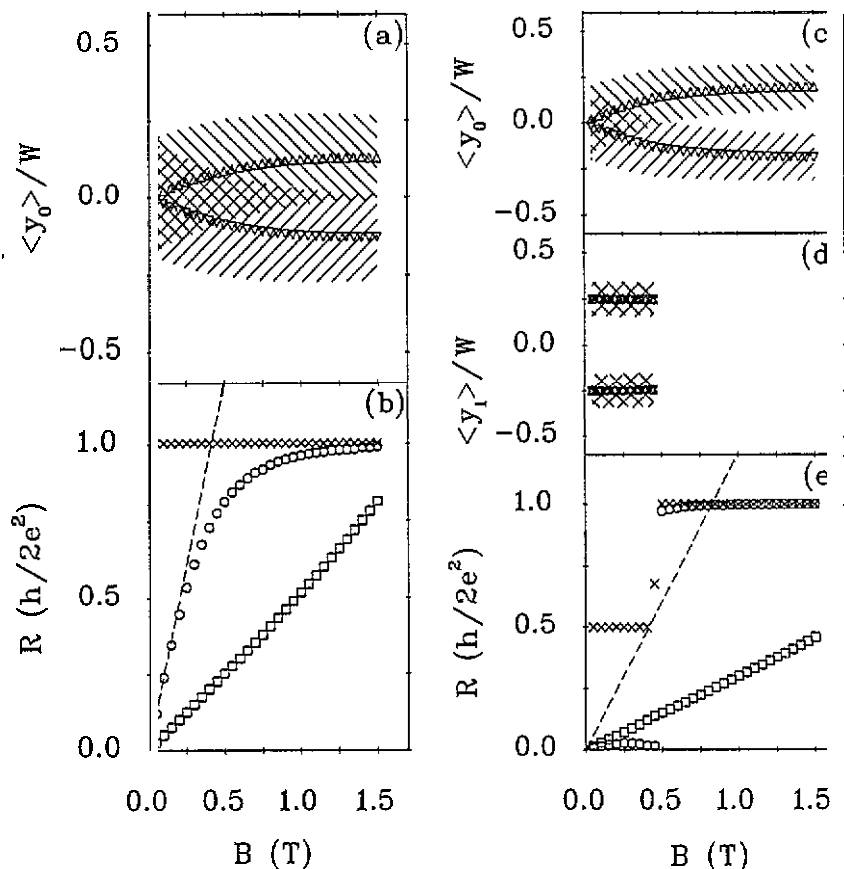


Figure 1. Plots showing overlap of the opposite-going wave functions in different subbands as a function of B and the corresponding R_L (crosses) and Hall resistances R_{EHP} (squares) and R_{LCP} (circles). Up (down) triangles refer to the average position of right- (left-) going wave functions and the cross-hatch lines sloping down to the right (left) mark the corresponding wave-function spread. The width of the wire is $W = 100$ nm and the electron densities are $n_s = 2 \times 10^{14} \text{ m}^{-2}$ in (a) and (b) and $n_s = 4 \times 10^{14} \text{ m}^{-2}$ in (c), (d), and (e). The broken lines show the classical Hall resistances.

shows that R_{LCP} is quenched when $B < 0.5$ T and figures 1(c) and (d) confirm that the quenching is associated with severe overlap of the $n = 1$ wave functions, while the $n = 0$ wave functions are separating as they did in figure 1(a). The broken lines in figures 1(b) and (e) show the behaviour of the classical Hall resistance. As soon as the second subband is depopulated, R_{LCP} jumps to the quantized value because the opposite-going $n = 0$ wave functions are separated at the two edges.

We see that the LCP at a wire edge is determined by the values there of the opposite-going electron wave functions of all of the occupied subbands. Increasing the overlap at the edges decreases the LCP difference between the edges. The singularity of density of states at the bottom of a subband enhances this effect enormously. In the limit, $B \rightarrow 0$, the left- and right-going wave functions coincide and the LCP difference across the wire is zero. For small B , there will consequently be almost complete quenching of R_{LCP} because the opposite-going wave functions of all the occupied subbands overlap heavily at the edges.

When the opposite-going wave functions of any one subband are separated, the level of quenching of R_{LCP} is reduced. Finally, when every pair of opposite-going wave functions is well separated, the LCP difference approaches the chemical potential difference between the two ends of wire and the R_{LCP} is almost exactly quantized.

We always suppose in the calculations described above that n_s is fixed. Consequently, when only the ground subband is occupied, the corresponding Fermi wave number k_{F_0} is also fixed. In that case, increasing B from zero simply separates the wave functions. On the other hand, when two subbands are occupied, increasing B increases k_{F_0} but *reduces* the Fermi wave number k_{F_1} in the second subband. For $n_s = 4 \times 10^{14} \text{ m}^{-2}$, $k_{F_1} \ll k_{F_0}$. Hence, when B is increased the $n = 0$ wave functions separate quickly but the $n = 1$ wave functions do not, with the result that R_{LCP} is quenched.

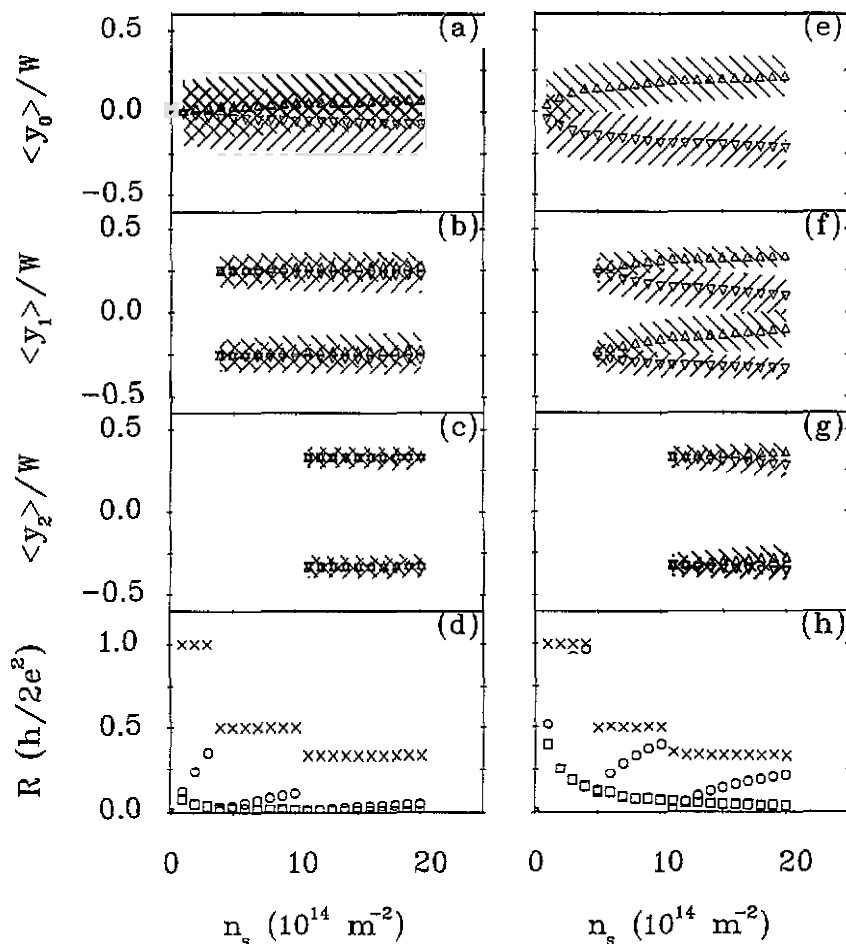


Figure 2. Plots showing the dependence on n_s of the opposite-going wave functions in different subbands and the corresponding Hall resistances. The width of the wire and the notation are the same as in figure 1; $B = 0.1 \text{ T}$ in (a)–(d) and 0.5 T in (e)–(h).

The behaviour when B is fixed and n_s is changed is also interesting. Results are shown in figure 2 for $B = 0.1 \text{ T}$ and $B = 0.5 \text{ T}$ in figures 2(a)–(d) and (e)–(h) respectively. When

$B = 0.1$ T the opposite-going wave functions of every occupied subband overlap heavily as shown in figures 2(a)–(c). Consequently, in figure 2(d) R_{LCP} is always small. When $B = 0.5$ T we see from figures 2(e)–(g) that the overlap between the opposite-going wave functions in each occupied subband is reduced, and the wave functions separate as n_s (and consequently k_{F_n}) increases. Consequently, R_{LCP} in figure 2(h) increases quickly with n_s as each subband is traversed.

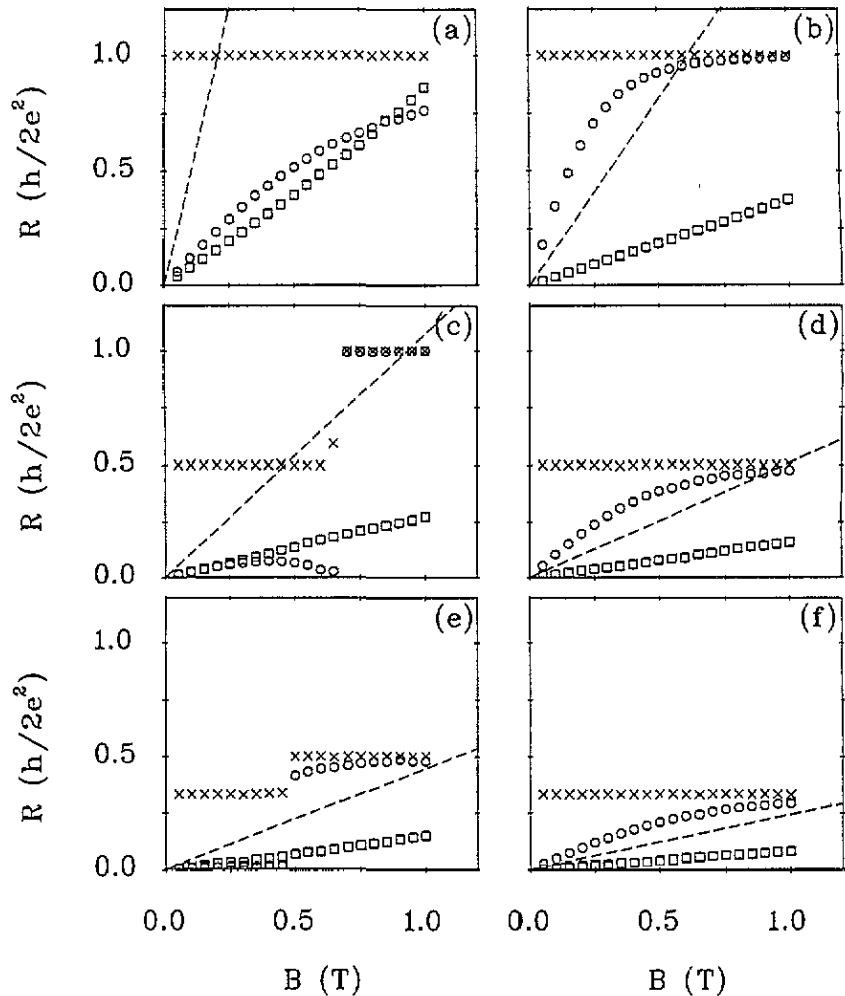


Figure 3. Plots showing R_{EHP} (squares), R_{LCP} (circles), and R_L (crosses) versus B for $n_s = 10^{14} \text{ m}^{-2} \times 1.0$ (a), 3.0 (b), 4.5 (c), 9.5 (d), 10.8 (e), and 19.8 (f). The width of the wire and the notation are the same as in figure (1). The broken lines show the classical Hall resistance.

We see from figure 2 that R_{LCP} is quenched intermittently as n_s varies. This effect has been seen experimentally [5] and theoretically in the strong-coupling case [13]. To investigate it in more detail we show in figure 3 plots of the various Hall resistances against B for several different values of n_s . The graphical notation is the same as in figures 1 and 2. In figure 3(a) $n_s = 1.0 \times 10^{14} \text{ m}^{-2}$. Only the ground subband is occupied and k_{F_0} is large enough to prevent overlap so that there is no quenching. This is also true in figure

3(b) for which $n_s = 3.0 \times 10^{14} \text{ m}^{-2}$. But, because k_{F_0} is now larger, R_{LCP} increases more rapidly towards $h/2e^2$. In figure 3(c) $n_s = 4.5 \times 10^{14} \text{ m}^{-2}$. Only the ground subband is occupied when $B > 0.7 \text{ T}$ but n_s is now large enough for the $n = 1$ subband to be occupied as well when $B < 0.7 \text{ T}$. We see that quenching sets in in this regime because k_{F_1} is small and the wave functions in the $n = 1$ subband overlap. In figure 3(d) we have increased n_s to $9.5 \times 10^{14} \text{ m}^{-2}$ to ensure that both subbands remain occupied for all B and both k_{F_0} and k_{F_1} are large enough to prevent significant overlap. Consequently, R_{LCP} is not quenched. In figure 3(e) $n_s = 10.8 \times 10^{14} \text{ m}^{-2}$ and three subbands are occupied when $B < 0.5 \text{ T}$. As would be expected, the quenching behaviour is similar to that shown in figure 2(c). Finally, in figure 3(f), we have increased n_s to $19.8 \times 10^{14} \text{ m}^{-2}$ so that all three subbands remain occupied for all B with relatively large Fermi wave numbers. The situation is similar to that shown in figure 3(d) and quenching is suppressed.

In summary, we find intermittent quenching of the QHR in a uniform ballistic quantum wire as n_s varies. The quenching is intrinsic and produced by overlap near the edges of the wire of opposite-going wave functions in the same *excited* subband. The overlap is strong at low B when n_s has a value which yields a small Fermi wave number in the uppermost occupied subband. The singularity of the density of states at the bottom of the subband greatly enhances this effect. No quenching is found when the singularity is omitted from the LCP formula [9, 10]. The calculations presented here are self-consistent. We find that both the intra- and inter-subband couplings produced by the Coulomb interaction play a part in determining the quenching behaviour of the QHR. Calculations which do not include Coulomb interaction show less overlap, weaker quenching, and reduced widths of the ranges of n_s in which quenching occurs.

The uniform quantum wire has a geometry which is simple enough to allow self-consistent calculations to be carried out relatively easily. However, measurements of the QHR of a wire are difficult because they require the insertion of non-invasive probes. For this reason the QHR is usually measured in (at least) a cross with four terminals. The fundamental reason for quenching in the cross is similar to that discussed here: mixing in the Hall voltage probes of the wave functions for electrons emerging from the current source and the current drain. In both cases it is geometry which produces the overlap or mixing: the narrowness of the wire in our calculations and, for example, rounded corners in a cross. In a wire we find that Coulomb interaction is an important factor in determining quenching behaviour. It is expected that this is also true in a cross and the implementation of self-consistent calculations in a cross geometry presents a challenging problem.

The authors wish to thank T Xiang for useful discussion. This work is supported by the SERC (Science and Engineering Research Council).

References

- [1] See, e.g., Reed M A and Kirk W P (ed) 1989 *Nanostructure Physics and Fabrication* (New York: Academic)
- Beenakker C W and van Houten H 1991 *Solid State Physics: Advances in Research and Applications* vol 44, ed H Ehrenreich and D Turnbull (New York: Academic) pp 1-228
- [2] Roukes M L, Scherer A, Allen Jr S J, Craighead H G, Ruthen R M, Beebe E D and Harbison J P 1987 *Phys. Rev. Lett.* **59** 3011
- [3] Ford C J B, Thornton T J, Newbury R, Pepper M, Ahmed H, Peacock D C, Ritchie D A, Frost J E F and Jones G A C 1988 *Phys. Rev. B* **38** 8518
- [4] Ford C J B, Washburn S, Büttiker M, Knoedler C M and Hong J M 1989 *Phys. Rev. Lett.* **62** 2724
- [5] Chang A M, Chang T Y and Baranger H U 1989 *Phys. Rev. Lett.* **63** 996
- [6] Timp G, Baranger H U, de Vegvar P, Cunningham J E, Howard R E, Behringer R and Mankiewich P M 1989 *Phys. Rev. Lett.* **60** 2081

- [7] Takagaki Y, Gamo K, Ishida S, Ishibashi K and Aoyagi Y 1988 *Solid State Commun.* **68** 1051
- [8] Kakuta T, Takagaki Y, Gamo K, Namba S, Takaoka S and Murase K 1991 *Phys. Rev. B* **43** 14 321
- [9] Peeters F M 1988 *Phys. Rev. Lett.* **61** 589; 1989 *Superlatt. Microstruct.* **6** 217
- [10] Akera H and Ando T 1989 *Phys. Rev. B* **39** 5508
- [11] Li Q and Thouless D J 1990 *Phys. Rev. Lett.* **65** 767
- [12] Ravenhall D G, Wyld H W and Schult R L 1989 *Phys. Rev. Lett.* **62** 1780
- [13] Kirczenow G 1989 *Phys. Rev. B* **39** 10452
- [14] Baranger H U and Stone A D 1989 *Phys. Rev. Lett.* **63** 414
Baranger H U, DiVincenzo D P, Jalabert R A and Stone A D 1991 *Phys. Rev. B* **44** 10637
- [15] Beenakker C W J and van Houten H 1989 *Phys. Rev. Lett.* **63** 1857
- [16] Geisel T, Ketzmerick R and Schedletsky O 1992 *Phys. Rev. Lett.* **69** 1680
- [17] Shepard K L, Roukes M L and Van der Gang B P 1992 *Phys. Rev. Lett.* **68** 2660
- [18] Engquist H-L and Anderson P W 1981 *Phys. Rev. B* **24** 1151
- [19] Landauer R 1987 *Z. Phys. B* **68** 217
- [20] MacDonald A H, Rice T M and Brinkman W F 1983 *Phys. Rev. B* **28** 3648
- [21] Chu D P and Butcher P N 1993 *Phys. Rev. B* **47** 10008
- [22] Büttiker M 1988 *IBM J. Res. Dev.* **32** 317; 1988 *Phys. Rev. B* **38** 9375
- [23] Entin-Wohlman O, Hartzstein C and Imry Y 1986 *Phys. Rev. B* **34** 921